STM JOURNALS

Current Trends in
Signal Processing

https://journals.stmjournals.com/ctsp

ISSN: 2277-6176 (Online)
ISSN: 2321-4252 (Print)
Volume 17, Issue 1, 2026
January–April
DOI (Journal): 10.37591/CTSP

Review CTSP

Spectral Mapping and Tracking Error of MBOC Signal and Wavelet-Based GNSS Receiver

Shubham Kumar Singh[1], Soumyo Nath Tripathy[1], Rintu Kumar Gayen[2], Debashish Chakravarty[3], Tamesh Halder[3,*]

Abstract

This research paper delves into the historical evolution and contemporary state of the art in navigation technologies, emphasizing the paramount importance of reliable positioning systems. Tracing the journey from ancient primitive methods to the present-day global navigation satellite systems (GNSS), with a focus on the global positioning system (GPS), the paper explores the diverse instruments and methods developed by civilizations throughout history to determine location and navigate effectively. The main objective of modern navigation technologies, particularly GPS and GNSS, is to provide users with accurate position, velocity, and time (PVT) information. The paper explains the trilateration principle used to calculate PVT parameters and explores the role of the Doppler shift in determining user relative velocity. The frequency plan and signal structure, including the use of L-band frequencies and modulation schemes, are detailed for GPS, GLONASS, and Galileo systems. The paper introduces the multiplexed binary offset carrier (MBOC) modulation scheme as a potential solution for second-generation radio navigation systems, addressing issues of robustness, interference, and improved tracking performance. The article also explores the properties of wavelets, focusing on the trade-off between time and frequency resolution. Affine wavelets, constructed through translation and dilation of a single function, offer flexibility in tiling the time- frequency plane, enabling diverse applications. The wavelet function is defined, and a reconstruction method is presented, emphasizing the importance of the admissible condition for the wavelet function. A discrete version of the wavelet is introduced, involving parameters that determine resolution in time and frequency. Multi-resolution analysis (MRA) for finite-energy signals is presented, emphasizing nested subspaces and orthonormal bases. The decomposition of L2(R) into subspaces and the introduction of orthogonal complement spaces facilitate a comprehensive understanding of wavelet theory without any sparse-based learning approach.

Keywords: Global navigation satellite systems (GNSS), global positioning system (GPS), position, velocity, and time (PVT), trilateration, Doppler shift, multiplexed binary offset carrier (MBOC), frequency plan, signal structure, wavelet, acquisition and tracking

***Author for Correspondence**
Tamesh Halder
E-mail: haldertamesh@iitkgp.ac.in

[1]Student, Department of Electronics and Communication Engineering, Institute of Engineering and Management, Kolkata, West Bengal, India
[2]Assistant Professor, Department of Electronics and Communication Engineering, Institute of Engineering and Management, Kolkata, West Bengal, India
[3]Professor, Department of Mining Engineering, Indian Institute of Technology, Kharagpur, West Bengal, India

Received Date: March 17, 2026
Accepted Date: March 19, 2026
Published Date: April 28, 2026

Citation: Shubham Kumar Singh, Soumyo Nath Tripathy, Rintu Kumar Gayen, Debashish Chakravarty, Tamesh Halder. Spectral Mapping and Tracking Error of MBOC Signal and Wavelet-Based GNSS Receiver. Current Trends in Signal Processing. 2026; 17(1): 50–65p.

INTRODUCTION

Since the evolution of wavelet theory, originating with Haar's orthonormal basis in 1910, a single function subject to discrete dilation and translation along the time axis has seen significant advancements in the last century. In 1985, Daubechies et al. discovered another basis, contributing to the foundation of wavelet theory. Concurrently with this, Gabor's time-frequency approach led to the short-time Fourier transform. IBM France's Estaban and Galand, in 1977, implemented a filtering method with low- and high-pass bands free of aliasing, laying the groundwork for wavelet theory on a biased prolate spheroid surface basis. Although a Finite Impulse Response (FIR) filter could not meet the criteria (this problem was solved by Smith and Barnwell in 1980), they laid the foundation of the present theory of wavelets as a Reisz basis. Affine wavelets, introduced by Grossmann and Morlet for oil exploration, provide effective signal decomposition. Daubechies, Meyer, and Mallat later constructed a comprehensive theory of time-scale approaches as a basis [1]. The paper explores the trade-offs inherent in time-frequency localization through Gabor and affine wavelets, highlighting the balance between frequency and time resolution. Mathematical foundations, including multi-resolution analysis, provide insights into orthonormal bases that offer varying resolutions in the time and frequency domains in GPS receiver applications.

The reliability of positioning systems is of utmost importance in the paradigm of contemporary navigation technologies. From ancient times, people used primitive ways to find desired locations and their route direction and navigate from one place to another. In this paper, we describe the current state-of-the-art navigation technology. Since the dawn of human civilization, people have designed, developed, and constructed many devices and methods (e.g., stars, the direction of the wind, and terrestrial points of interest) to locate their position on the face of the earth and to find their way back home. The Minoan civilization of Crete navigated the seas over 130,000 years ago using the positions of celestial bodies. Positioning has always been a vital requisite of exploring new lands, improving cultural or daily conditions, and being defensive or offensive in warfare; thus, in short, sustaining and evaluating the human species in a hostile nature. During the Qin dynasty (221–206 B.C.), the magnetic compass, an ancient Chinese invention, was first used as a fortune-telling tool. Later, the compass was used as a navigational device on ships between 850 and 1050 A.D. With time and the development of instruments in navigation, it has become an attractive field. A ‘Kamal’ is a celestial navigation device that allows the determination of latitude. It was primarily used by Arabs during the Islamic Golden Age. The sextant was a better navigation instrument in the mid-18th century. It measures the elevation angle between a heavenly body and the skyline. In the late 18th century, John Harrison’s life’s work resulted in a marine chronometer.

METHODOLOGY

The main objective of using GPS or GNSS is to obtain the position, velocity, and time (PVT) of the user with a certain reference frame [2]. Practically, when we measure the range, we need three satellites for coordination and another one for clock bias. The phase of the incoming signal is measured by correlating the incoming signal with a local receiver-generated replica. With four satellites and known distances from Earth, the longitude, latitude, altitude, and correction of the user’s clock bias can be calculated. The basic principle of finding the PVT is ‘trilateration’ (Figure 1) [3], and the receiver needs to solve the so-called ‘navigation equation’ for position-related parameters using at least four satellites. The Doppler shift in the received signal can also be measured to determine the relative velocity of the user.

The whole GPS is based on three major segments. These are:

Space Segment

GPS space segment consists of:

1. *GPS orbit configuration and multiple access:* Satellite constellations must allow simultaneous multiple-user access to measure the pseudo-range of any location on the globe using four or more satellites. The position of satellites must be such that the mutual interference decreases to zero, thus providing multiple access signaling. The selection of satellite altitude has several effects from the user’s perspective. A higher orbit altitude covers a greater fraction of the Earth with a single satellite. The power flux density on Earth is nearly independent of the orbit altitude because the selection of the antenna beam width can be based on user requirements.

   A low-orbit altitude comprises short-time visibility and a larger Doppler shift, and satellite-to-satellite signal handover allows increased signal acquisition time in the receiver. The space vehicle or GPS satellites, with an orbital period of 12 hours sidereal time on orbital planes, produce a ground track or projection on Earth's surface that repeats over and over. The satellites or the Space Vehicle (SV) make use of solar energy to move around the Earth twice a day. The 14 solar panels are constantly adjusted to direct the solar cells toward the Sun and the antennas toward the Earth. For GPS, the longitude crossing at the equator is maintained within the GPS-control segment. Orbiting at an altitude of approximately 20,162.61 km, an average of 10 satellites are visible within the field of view in a clear sky (Figure 2).

2. *Satellite Payload:* The satellite transmits precisely timed GPS signals, mostly at the L1 frequency centered at 1575.42 MHz and the L2 frequency centered at 1227.6 MHz. The signal consists of navigation data (clock bias information and satellite position data), pseudo-random noise (PRN) code, and carrier signal. The navigation data uploaded from the control segment is stored in the satellite's memory chip to provide a navigation data stream.

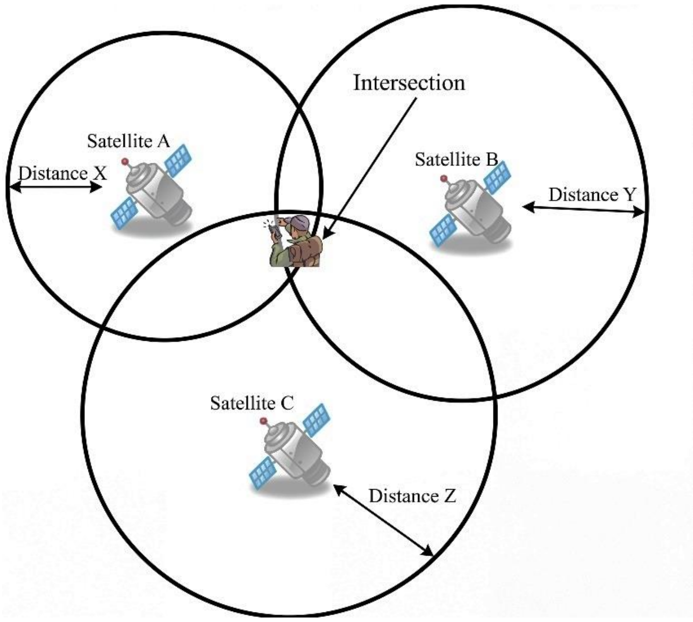

Figure 1. Intersection among coverage areas of three satellites and pinpoint the user's position.

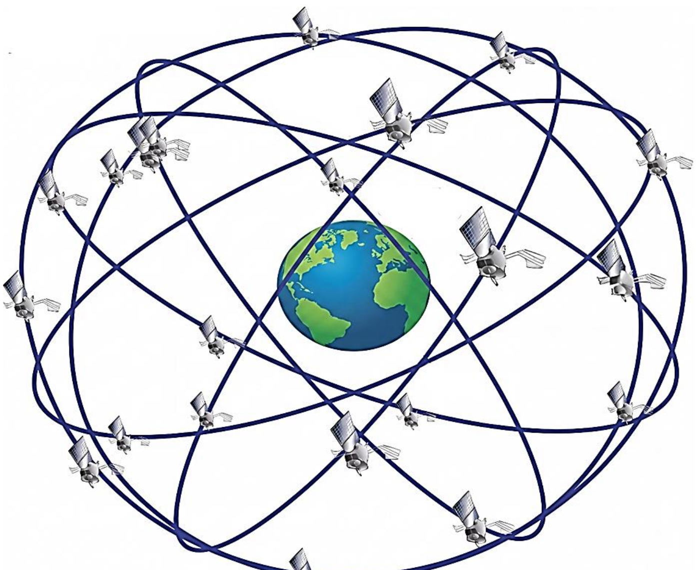

Figure 2. GPS satellite constellation: 24 satellites in six orbital planes, 55° inclination, and 20,200 km altitude at FOC.

The navigation data contains ephemeris data regarding satellite orbit, the exact position in that orbit vs. time, and clock correction data (to calibrate the offset between the satellite clock and GPS time). These data were uploaded using the S-band telemetry and tracking command system (TTC) (Figure 3). Each satellite carries redundant atomic oscillators. This type of oscillator is highly stabilized because it uses either rubidium or cesium atoms in the gaseous form [2]. In the TTC system, an appropriate frequency synthesizer along with an atomic clock is used to synchronize GPS signal generators and control the precision of the center frequencies of the two L-band radio frequencies. The signals are then amplified and filtered to remove the signal power outside the allocated bandwidth. One of the GPS clock errors is selective availability, which is a clock dither in navigation data that restricts non-military access to achieve the highest accuracy of the system.

3. *Augmentation of GPS:* GPS satellites are augmented with signal sources of various ranges that are situated on Earth. Ground transmitters or pseudolites transmit a special form of integrity beacon with a GPS signal. Wide-area differential ground stations transmit correct information to the equipped GPS receivers for further accuracy.

Control Segment

This segment maintains the orbit, constellation, satellite clock, and payload. It also generates navigation data and uploads it to each satellite. So, it is mainly responsible for the monitoring of the health and status of space segments through infrequent commanded maneuvers. Generally, in the case of GPS, the control segment comprises five monitoring stations, four ground antenna upload stations, and one master control station. Each of the five monitoring stations had redundant GPS tracking receivers and multiple cesium reference oscillators. These stations provide the measurement of code delay and carrier phase delay for each satellite signal, and this information is uploaded to the master control station. The ground antenna section sends navigation data to the telemetry-tracking and command unit.

User Segment

This segment consists of antennas and receivers that determine the position, velocity, and time of users via satellite transmissions. As the user receiver operates passively (it does not transmit any signal), the space segment provides many users at a time.

Frequency Plan

For downlink transmission, the space segments use L-band frequencies. The GPS uses L1, L2, and L5 bands (center frequencies 1575.42 MHz, 1227.60 MHz, and 1176.45 MHz, respectively) for transmission [4]. Galileo also transmits navigation signals at the L band with different frequencies that are interoperable with GPS transmission frequencies and are indicated as E1, E6, E5a, and E5b bands (center frequencies 1575.42 MHz, 1278.75 MHz, 1176.45 MHz, and 1207.14 MHz, respectively). Figure 4 shows the PSD of the Sine subcarrier BOC (1, 1) [dotted line] and the Cosine subcarrier BOC (1, 1) [solid line]. Galileo frequency bands were selected for the RNSS. E1, E5a, and E5b are also selected for Aeronautical Radio Navigation Services (ARNS), deployed by Civil Aviation users, and allow safety-critical applications. The wider bandwidths of the E5 and L5 bands are advantageous for the tracking precision of the receiver [5].

It should be noted that all signal components are derived from a highly stabilized atomic clock that generates a pure sine wave at a fundamental frequency of f0 =10.23 MHz. Figure 5 shows the PSD of BOC sin (15, 2.5) and BOC cos(15, 2.5) [here, the frequency center at the bottom axis is considered zero]. The fundamental frequency yields the two L-band carrier frequencies L1 and L2 (f0 154=157542 MHz and f0 120=122760 MHz), respectively. In the case of the GLONASS-allocated frequency spectrum, the L1 band (center frequency 1598-1605 MHz with 18 MHz bandwidth), L2 band (center frequency 1243-1248 MHz with 16 MHz bandwidth), and L5 band (center frequency 1198-1203 MHz with 14 MHz bandwidth) are designated (Figure 6). Figure 7 shows the PSD plots of BOC (1, 1), BOC (6, 1), and MBOC (6, 1, 1/11) [here, the frequency center on the bottom axis is considered zero].

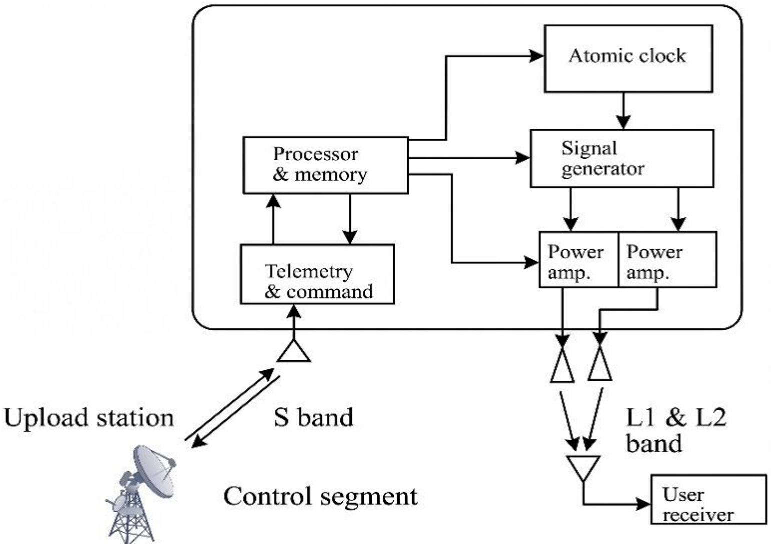

Figure 3. GPS satellite payload functional block diagram.

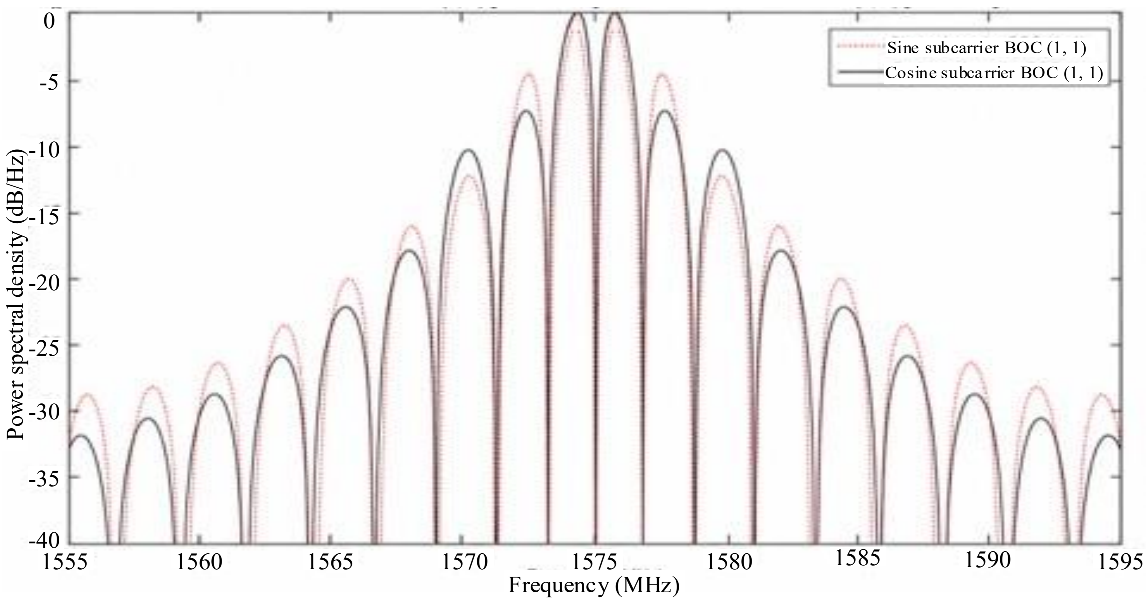

Figure 4. PSD of Sine subcarrier BOC (1, 1) [dotted line] and Cosine subcarrier BOC (1, 1) [solid line].

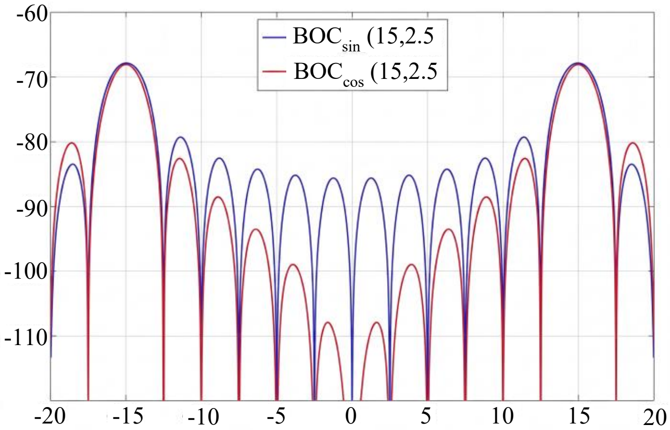

Figure 5. PSD of BOC sin (15, 2.5) and BOC cos(15, 2.5) [here the frequency center at the bottom axis is considered zero]

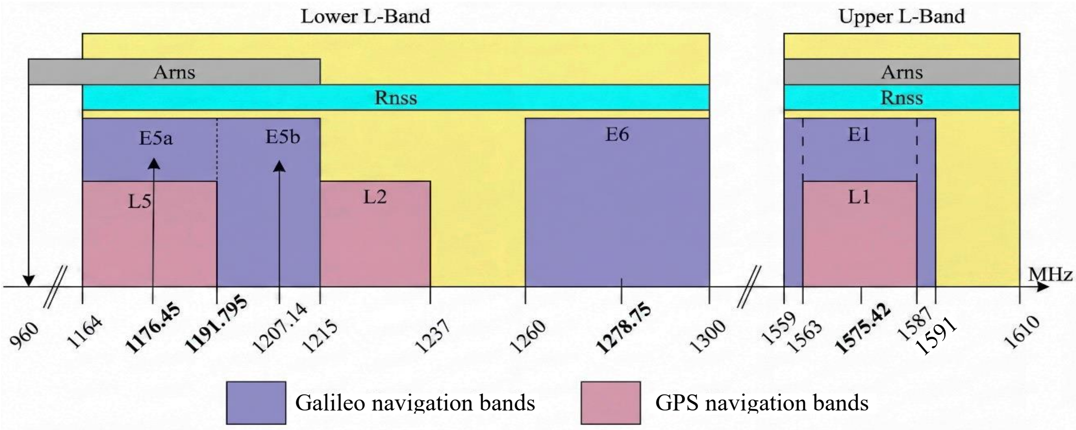

Figure 6. Galileo and GPS frequency plan [6].

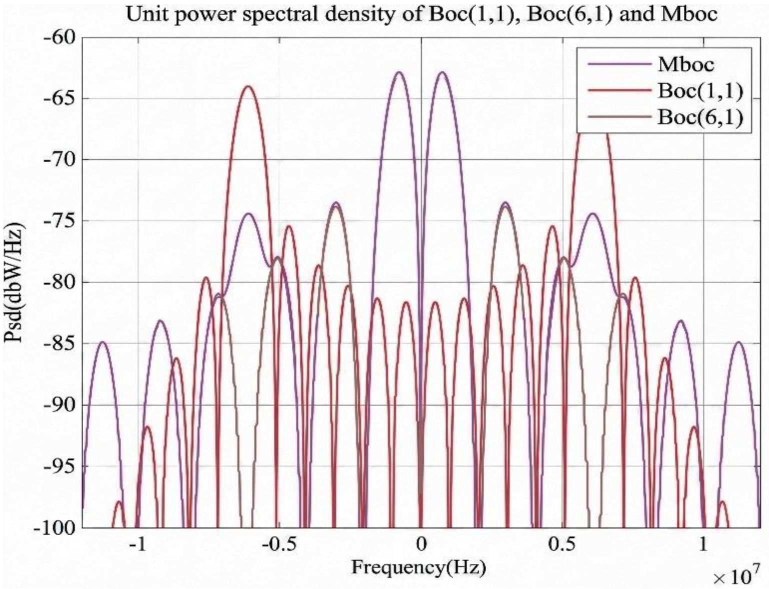

Figure 7. PSD plots of BOC (1, 1), BOC (6, 1), and MBOC (6, 1, 1/11) [here, the frequency center on the bottom axis is considered zero]

Structure and Modulation Schemes for GNSS (GPS, GLONASS, and Galileo) Signals

The space segments of GPS and GLONASS transmit two codes (C/A and P) on two frequencies, namely the L1 and L2 bands. Some GPS satellites also transmit military codes (M codes) on both the L1 and L2 channels. In addition, the L5 band (center frequency 1176.45 MHz) for GPS and the L3 band (center frequency 1207.14 MHz) for GLONASS were assigned (Figure 8). In the near future, a new civil signal, L1C, is planned for the GPS. The fundamental differences between GPS, GLONASS, and Galileo are spectrum allocation (i.e., center frequency and bandwidth) and installed techniques used for the recognition of satellites of certain systems. To allow multiple satellites to access the same receiver (i.e., Multiple Access), three main techniques are used, namely Frequency Division Multiple Access (FDMA), Time Division Multiple Access (TDMA), and Code Division Multiple Access (CDMA) (Figure 9). In the GPS and Galileo programs, the CDMA technique is used with distinct PRN codes, modulation techniques, and bandwidths, but all satellites can transmit at the same frequency. The TDMA technique, which can be characterized by multiplexing of different signals with certain time slots, is also used in both systems (GPS and Galileo) depending upon their band compatibility and interoperability. However, the FDMA technique is mainly used in the GLONASS system. In this case, each satellite is identified by its transmitted frequency, and all satellites use the same PRN code. Thus, the receiver technology of the GPS and Galileo systems is more sophisticated in terms of high memory and computation requirements for different PRN codes (Figure 10).

The navigation data are added together with the carrier frequency through multiplication, which is called "modulation." Various types of modulations exist that provide optimum data rates according to their assigned bandwidth (Figure 11). To emphasize the spectrum shape (for better acquisition and tracking performance), the navigation data rate is set lower (50 bps for GPS and 250 bps for Galileo). The modulation is selected based on the performance and architecture of the practically realized communication system. In the case of GPS, the navigation message is a continuous data stream transmitted at a rate of 50 bits/second [2]. It is transmitted by satellite on the L1 data link and consists of a bit stream of ones and zeros. The message is divided into logical units called 'frames.'

A superframe contained 25 frames with a duration of 12.5 min (Figure 12). The length of each frame is 1500 bits, and each frame takes 30 s for transmission. Each frame has 5 sub-frames with a length of 300 s. Each subframe contains 10 words of 30 bits each. Each starts with a pair of telemetry words (TLM) and handover words (HOW). HOW is transmitted after the TLM word is transmitted. The TLM consists of an 8-bit preamble (10001011), and the HOW contains a 17-bit Time of Week (TOW). In addition, there are eight data words. Each word has a parity in each frame. In each word, 6 bits are used for parity, and the other 24 bits are data bits. Two non-information-bearing bits (23 and 24) of the words are used for parity computation. The first three subframes repeat every 30 s and consist of the clock offset time-of-applicability and ephemeris time-of-applicability. The last two subframes repeat every 12.5 min and consist of Almanac and Ionospheric data.

The PRN codes that are necessary for the recipe of signal generation in navigation systems are fundamental to identifying satellites as well as defining the functionality of the receiver. PRN codes are required for time measurement (Figure 13). GPS and Galileo are used for satellite identification, but the GLONASS system uses various frequencies to identify satellites. Generally, a code is characterized by the shape of its autocorrelation and cross-correlation. The autocorrelation shape should have an abrupt high peak, which clarifies the time delay of the signal in the receiver unit. The cross-correlation should have a zero-response curve to maintain the correct identification of satellites and mitigate inter-satellite interference. Cross-correlation is an inherent interference caused by modulation techniques.

In 1960, Gold conducted research on codes, where combinations of linear feedback shift registers of various lengths produced different PRN codes. Initially, two different PRN codes were used in both GPS and GLONASS, namely the Coarse Acquisition (C/A) code and P code. The GPS C/A code rate is 1.023 MHz, and the chip length is 1023, whereas the GLONASS C/A code rate is 0.511 MHz, and the chip length is 511. The P code is 10 times longer than the C/A code in the GPS and GLONASS systems. For example, the GPS P-code is 266 days long with a code rate of 10.23 MHz. The number of chips was more than 2.35×10^{14} (Figure 14). Furthermore, the chip sequence is periodically reset at midnight every Saturday to prevent the use of unauthorized services. The encrypted version of the P code is the Y code, which allows for additional protection. The Galileo code has a similar shape, although its length is longer than that of the traditional GPS C/A code. The PRN codes of Galileo are described in the Galileo Open Service Interface Control Document [2]. Hence, the aforementioned paragraphs describe the signal structures of the three major navigation systems and multiple access methods.

As we had already discussed, the modulation scheme, spreading sequence, and data message are the governing factors of the signal prototype [7]; the questions about the construction of the spreading sequence and the modulation scheme remain unanswered. New signals must coexist with the planned present and future signals in the allocated spectrum band. It should offer greater robustness against RF interference from existing and newly deployed systems. Apart from the backward compatibility issue, it should provide a marked improvement in performance in code tracking, allowing shorter integration times and flexibility in the design of carrier tracking. However, it is also expected that the new modulated signal must have better accuracy in noisy channels caused by multipath interference errors. The new generic receiver should operate without relying on discriminator designs because robust discriminators provide poorer performance when no multipath occurs. The new generation requires a

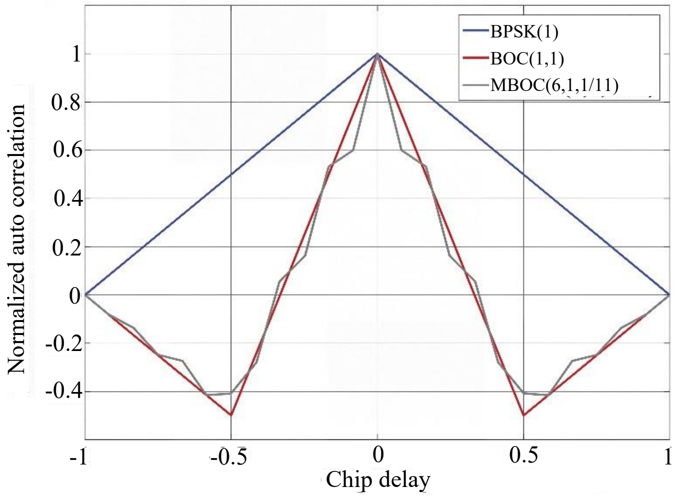

Figure 8. Normalized autocorrelation function shape of BPSK, BOC, and MBOC.

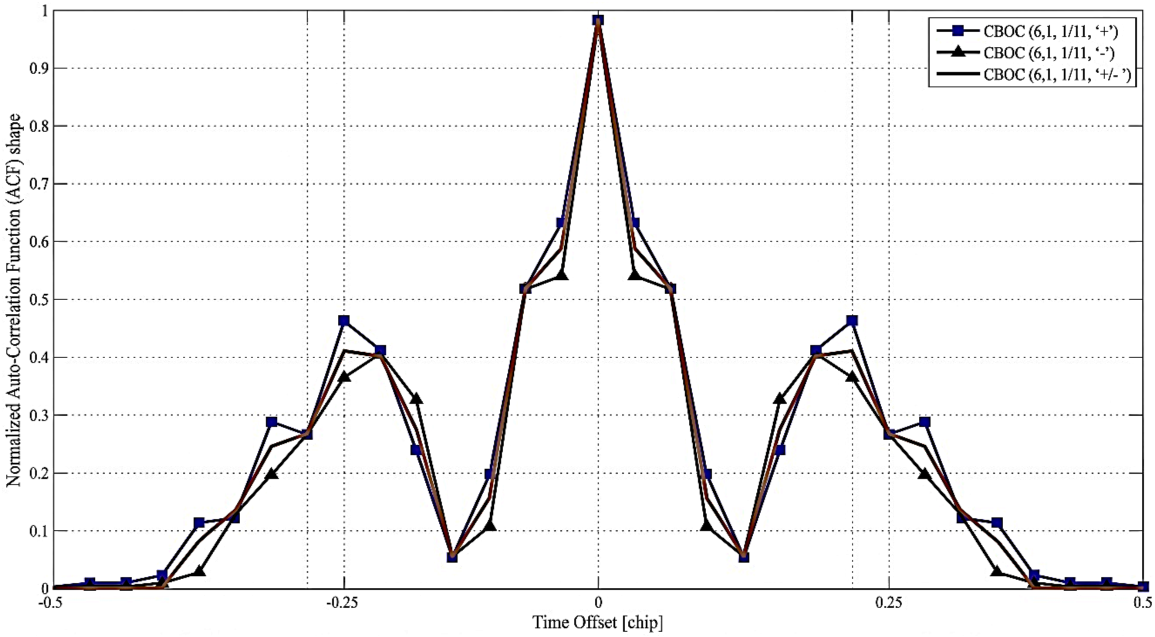

Figure 9. Normalized Auto-correlation function shape of CBOC (6,1,p, +), CBOC (6,1,p,-), and CBOC (6,1,p,+/-).

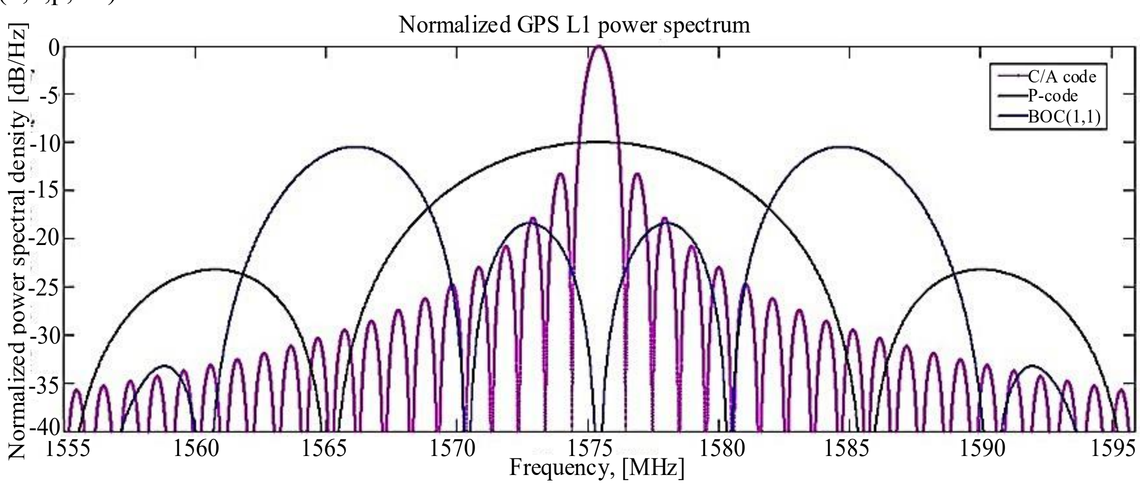

Figure 10. Normalized GPS L1 and L2 spectrum of C/A code, P-code, and BOC (1, 1).

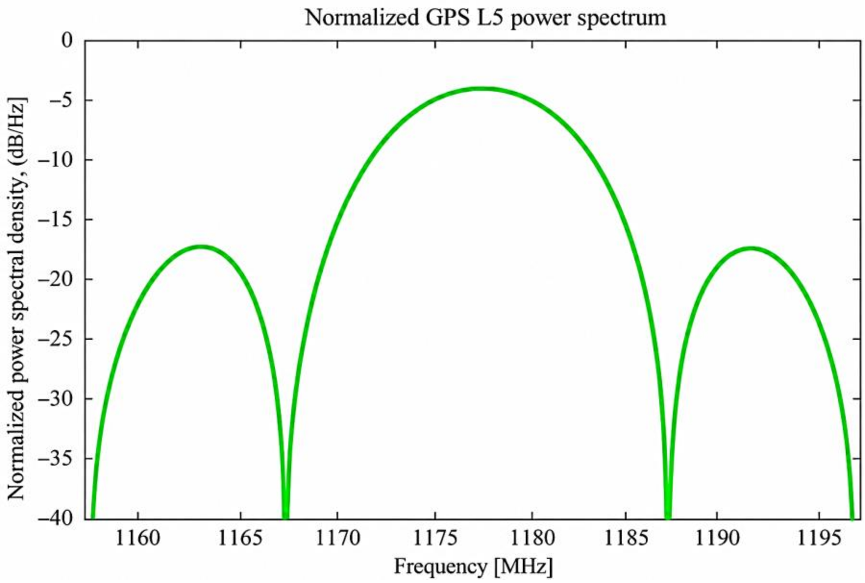

Figure 11. Normalized GPS L5 spectrum of BPSK (10.23 MHz).

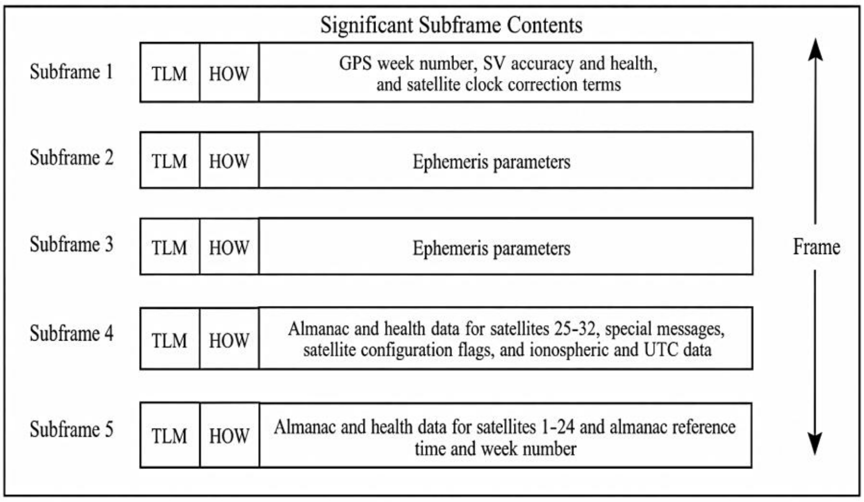

Figure 12. Navigation message content and format overview.

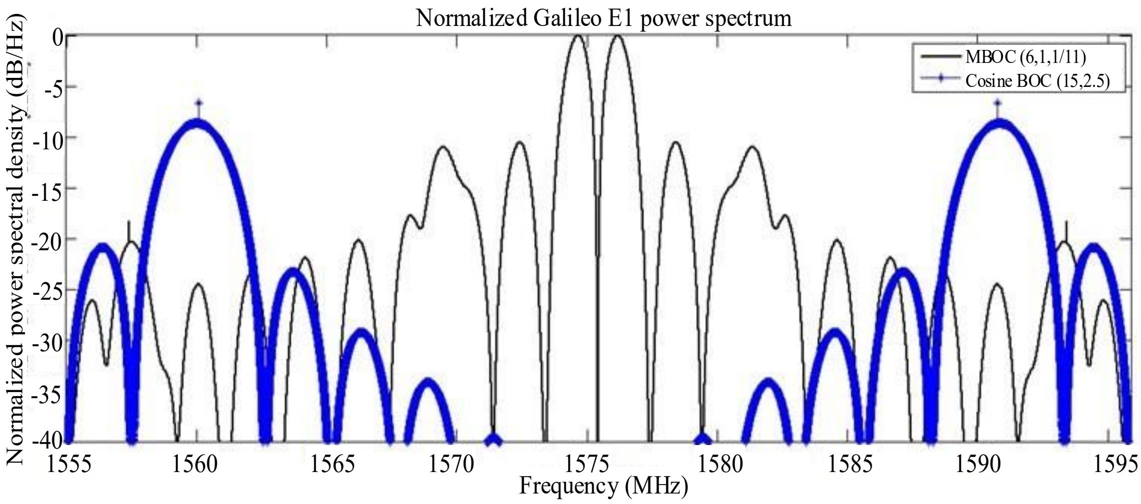

Figure 13. Normalized Galileo E1 spectrum.

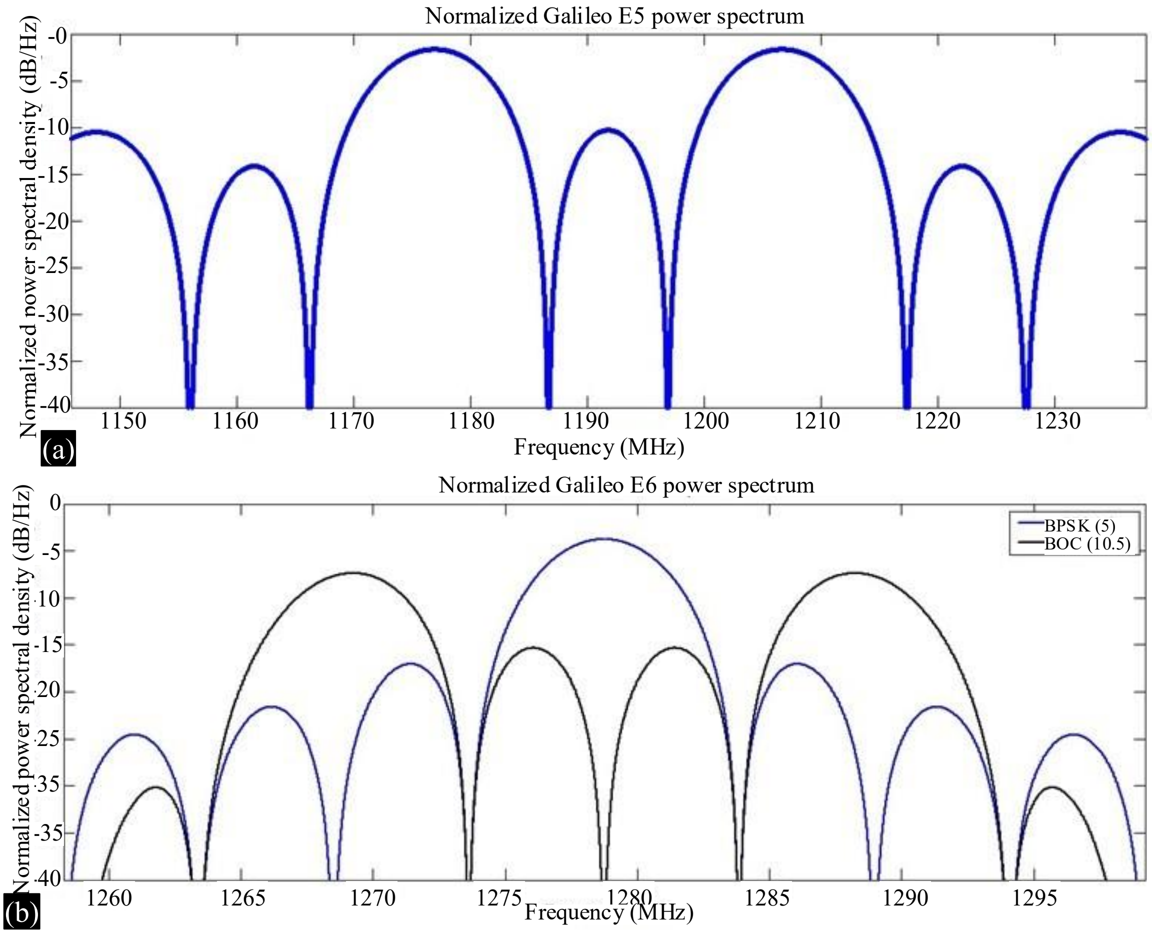

Figure 14. (a) and (b) Normalized GPS L1 band and Galileo E1 band spectrum allocation.

shorter integration time in the tracking loops. With these parameters, the new signal must provide greater channel capacity for the transmission of more signals at a time. The data and pilot signals were transmitted at different power levels. However, we must ensure that we do not unduly degrade the weaker signals. Therefore, a new modulation scheme is required. One such modulation scheme that enriches the transmitted signal with the above-described qualities is the Multiplexed Binary Offset Carrier (MBOC) [8]. The aforementioned performance parameters of a second-generation radio navigation system are being studied and simulated in the MATLAB environment for MBOC signals and further compared with Binary Phase Shift Keying (BPSK) and Binary Offset Carrier (BOC) signals.

Application of Discrete Wavelet at the Acquisition Module of the Receiver

The culmination of this exploration is the presentation of the fast discrete wavelet transform implementation, showcasing the practical application of wavelet theory in signal processing. In essence, this study provides a concise overview of the historical milestones and mathematical intricacies of wavelet theory, offering insights into its evolution and practical utility in signal processing. Figure 15 shows the PRN code offset and Doppler frequency offset at the acquisition module of the GNSS receiver.

Figure 16 illustrates the fundamental characteristics of the Gabor wavelets and their representation in the time-frequency plane. Gabor wavelets, introduced by Dennis Gabor, play a crucial role in signal processing, offering a localized approach in the time and frequency domains. This figure provides insights into the structure of the Gabor wavelet and its associated time-frequency plane representation.

Simultaneously, the time-frequency plane representation, often referred to as a spectrogram, is presented alongside the Gabor wavelet. This representation vividly illustrates how the frequency content of the wavelet changes with time. The horizontal axis corresponds to time, and the vertical axis represents frequency. The intensity of the color or shading at a particular time-frequency point indicates the strength or magnitude of the signal at that specific combination of time and frequency.

In the time-frequency plane, the Gabor wavelets exhibit a trade-off between time and frequency localization. While the central lobe provides good temporal localization, sinusoidal modulation results in a spread of frequency content. This inherent duality is a key characteristic of Gabor wavelets and is crucial for understanding their applicability in capturing both rapid changes in the signal amplitude and varying frequency components.

Figure 17 illustrates the fundamental concept of affine wavelets, offering a visual representation of their time-frequency plane. Affine wavelets are constructed through discrete translation and dilation processes applied to a single function or window. This figure serves to elucidate the diverse tiling possibilities achievable in the time-frequency domain, providing graphical insight into the behavior of affine wavelets.

In the graphical depiction, the horizontal axis typically represents time, and the vertical axis represents frequency. Each curve in the figure corresponds to an affine wavelet, and the arrangement shows the impact of variations in translation and dilation on the wavelet shapes and positions. The distinct patterns and placements of these wavelets emphasize the versatility of the affine wavelets in adapting to different scales and locations within the time-frequency plane.

Moreover, the figure visually communicates the trade-off inherent in the time-frequency resolution achieved by the affine wavelets. At lower frequencies, the wavelets exhibit a good frequency resolution and capture variations with precision. Conversely, at higher frequencies, the wavelets prioritize a good time resolution, enabling accurate localization in the temporal domain. This graphical representation is crucial for understanding how the properties of affine wavelets can be leveraged to address specific requirements in signal analysis, depending on the application needs and characteristics.

Figure 18 presents the implementation details of the Fast Discrete Wavelet Transform (DWT), a crucial aspect of the time–frequency analysis methodology using wavelets. The figure illustrates a schematic representation of the process, highlighting the use of high-pass and low-pass filters to achieve an efficient wavelet transformation.

The following expands on the key elements depicted in Figure 18.

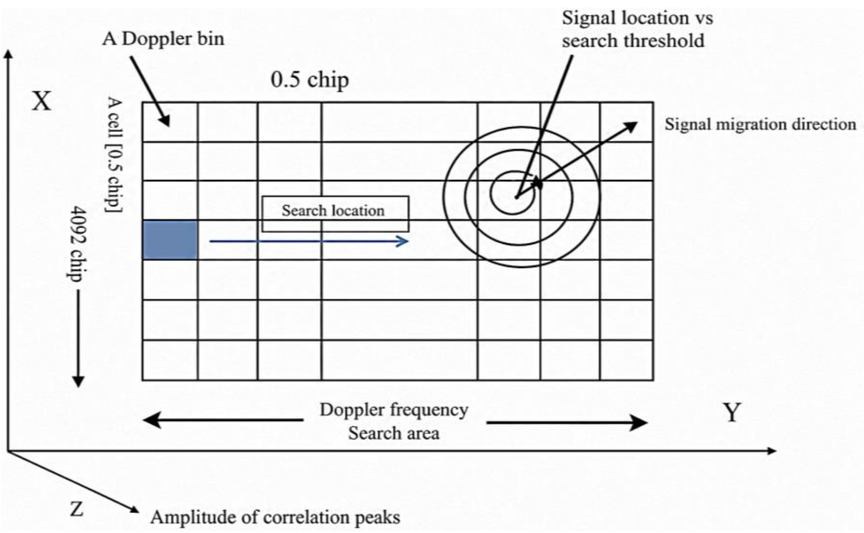

Figure 15. Finding peak location in Doppler frequency (125 Hz spacing) in Y axis and Code phase delay (0.5 chip: 1023*6/(12*1.023E6) = 0.5 msec).

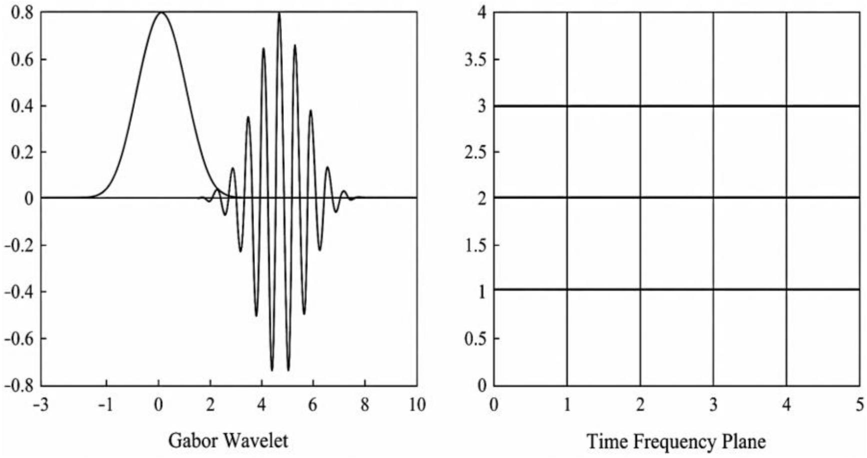

Figure 16. Gabor wavelet and its time-frequency plane representation.

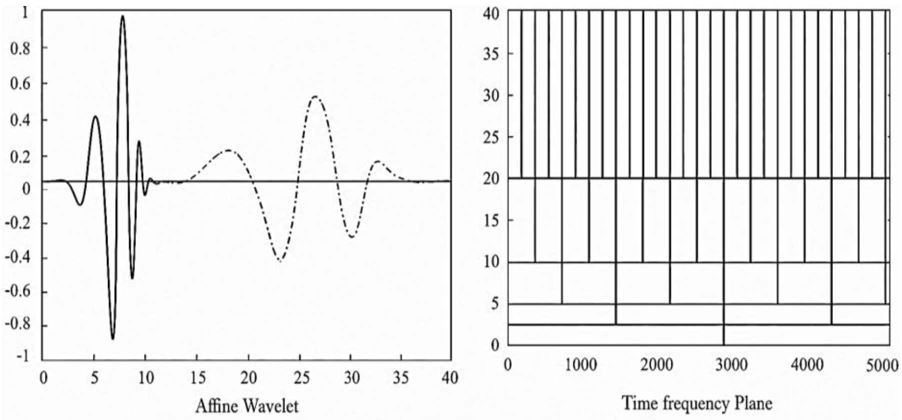

Figure 17. Affine wavelet and its time-frequency plane representation.

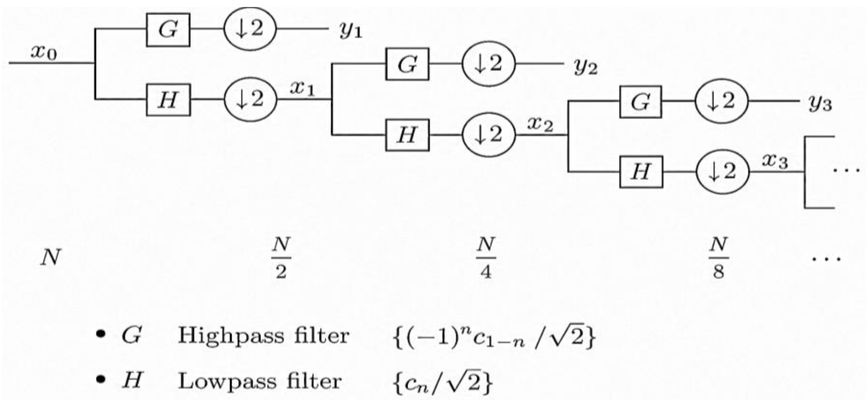

Figure 18. Fast discrete wavelet transform implementation using a set of high-pass and low-pass filters.

High and Low Pass Filters (G, H)

The figure shows two types of filters: a high-pass filter (G) and a low-pass filter (H). These filters are essential components of the wavelet transform process. High-pass filters allow the passage of high-frequency components while attenuating the low-frequency components. Conversely, low-pass filters allow the passage of low-frequency components while attenuating the high frequencies.

Sub-Sampling

After applying the high-pass and low-pass filters, the resulting signals were subsampled. Subsampling involves reducing the sampling rate of a signal, typically by selecting every alternate sample. The sub-sampled signals were further processed in subsequent stages, contributing to a multi-resolution analysis.

Iterative Process

The figure suggests the iterative nature of the wavelet transform. After each stage of high-pass and low-pass filtering, the resulting signals underwent additional rounds of filtering and subsampling. This process continues iteratively until the desired level of decomposition is achieved. Each iteration contributes to a different resolution level in the time-frequency domain.

Signal Reconstruction

The high- and low-pass signals obtained through the iterative process, along with the original low-pass term, collectively contribute to the reconstruction of the original signal. The reconstruction process is crucial for maintaining the integrity of the original signal while extracting information at various scales.

Time Complexity Analysis (O(N))

Figure 18 illustrates the efficiency of the Fast Discrete Wavelet Transform by illustrating a time complexity of O(N). This complexity implies that the computational effort increases linearly with the size of the input signal (N), making the algorithm particularly well-suited for real-time applications.

The application of discrete wavelet transform (DWT) in signal processing offers a versatile approach to address challenges such as computational complexity, noise interference, and signal detection in various scenarios. In our approach, we leverage wavelet decomposition to reduce the signal length, subsequently applying the Fast Fourier Transform (FFT) for correlation purposes [8]. However, it is noted that the wavelet reconstruction in this system leads to a lower Signal-to-Noise Ratio (SNR), resulting in potential ambiguity in noisy environments.

In an alternative strategy, a wavelet-based denoising method is employed to achieve a higher SNR during signal acquisition [9]. Here, the wavelet transform is applied after the FFT operation, allowing for the mitigation of interference and other noise during signal reconstruction. The use of wavelet basis functions is effective for decomposing the signal, thereby facilitating noise reduction.

Our focus on reducing computational complexity guided our methodology, leading to the adoption of a single-level wavelet decomposition on the received signal, bypassing intermediate frequency processing. Specifically, the local Pseudo-Random Noise (PRN) code and the approximation coefficients (obtained from the low-pass filter output) of both signals undergo correlation using FFT. The correlated output is then transformed back to the original signal length using an inverse discrete wavelet transform.

RESULTS AND DISCUSSION

In our simulation, we explore the Haar wavelet and the Cohen–Daubechies–Feauveau (CDF) wavelet, which is a biorthogonal wavelet [1]. The results, as depicted in Figure 19 (comparison of different methods: standalone FFT; joint DWT and FFT; joint CDF and FFT) during the acquisition process, reveal that very little degradation occurs in the computed ratio of the 1st maximum to 2nd maximum peaks in the code delay Doppler bin, even after a significant C/N0 of 30.5 dBHz. This observation is crucial because it indicates that setting a threshold for peak detection is unnecessary.

The joint use of wavelet decomposition and FFT in our approach showcases the efficacy of this hybrid method in improving signal processing outcomes, particularly in scenarios with high noise levels. The choice of wavelet basis functions, such as Haar and CDF, contributes to the adaptability and robustness of the method in acquiring signals with enhanced SNR and reduced computational complexity (Figure 20).

Affine wavelets are shown to achieve good frequency resolution at low frequencies and good time resolution at high frequencies. This flexibility allows for a trade-off between time and frequency resolution based on the specific requirements of the application. The mathematical framework for wavelet analysis is presented, including the definition of wavelet functions, wavelet transforms, and signal reconstruction using wavelet coefficients.

The utilization of wavelet basis functions, including Haar and Affine wavelets (Cohen- Daubechies-Feauveau wavelets, i.e., CDF wavelets), is also elucidated in the context of noise reduction and denoising methods. Moreover, the joint processing of wavelet decomposition and the Fast Fourier Transform (FFT) for correlation emerges as a pivotal approach, showcasing its potential for improved signal detection even in environments with elevated noise levels. The historical context, theoretical foundations, and practical applications of wavelets have been seamlessly integrated. Affine wavelets, Fast Discrete Wavelet Transform, and the strategic application of wavelet decomposition and reconstruction collectively provide a robust framework for signal processing. This hybrid approach stands out for its efficiency, adaptability, and efficacy, providing valuable insights for practitioners navigating the intricacies of signal analysis and noise mitigation.

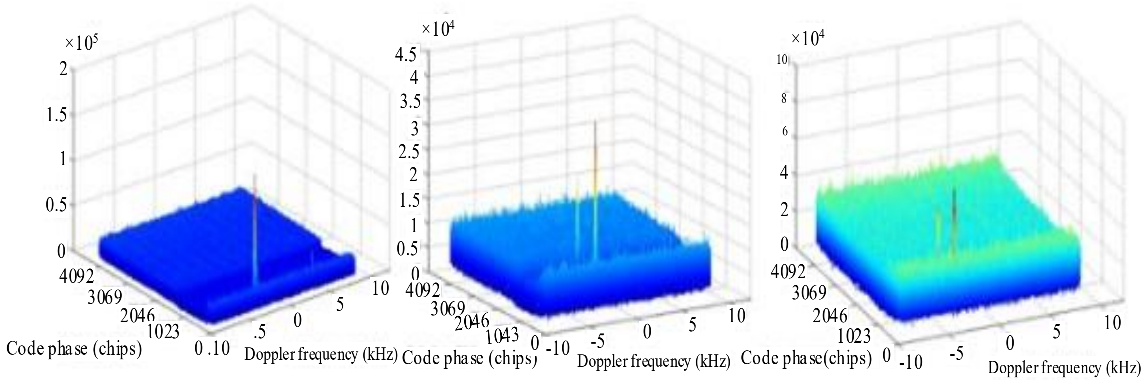

Figure 19. Acquisition peak in (a) single path channel, C/N0 = 46 dBHz, BW = 4 MHz; (b) and (c) represent multi path channel at C/N0 = 40 dBHz, 55 dBHz respectively with BW of 4 MHz and 2nd path signal gain is-1 dB from LOS.

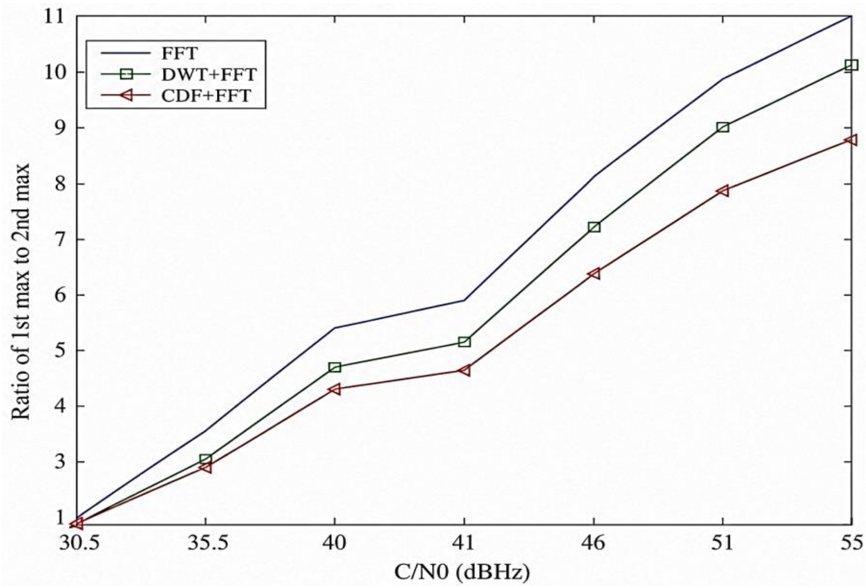

Figure 20. Comparison of different methods (standalone FFT; joint DWT and FFT; joint CDF and FFT) estimated ratio of the highest peak to the 2nd highest peak in the acquisition process (after 30.5 dBHz C/N0, the signal is detected).

The authors discuss the discrete version of wavelets, highlighting the role of parameters such as m and n in determining the time and frequency resolution. The concept of multi-resolution analysis (MRA) for finite energy signals is introduced, involving nested subspaces {Vm} with properties that facilitate signal decomposition, compared to other techniques where signal reconstruction in degraded SNR [10] and reducing PRN code offset and Doppler frequency offset bins [11] on the BPSK acquisition section of GNSS receiver units.

This study outlines the decomposition of the function space L2(R) into nested subspaces and discusses the relationship between these subspaces and dilation by powers of 2. In the final section, the authors report that very little degradation occurs in the computed ratio of 1st maximum to 2nd maximum peaks in the code delay Doppler bin, indicating the effectiveness of the chosen wavelet bases. The use of these wavelets is justified based on the observed results, and the authors conclude by emphasizing the importance of the chosen wavelet basis in achieving successful signal processing outcomes.

CONCLUSION

This paper emphasizes the crucial role of positioning systems in today's navigation technologies, highlighting the transition from primitive methods to sophisticated GPS and GNSS systems. The narrative traces the development of key instruments and inventions, such as the magnetic compass, marine chronometer, and utilization of satellites for navigation.

A detailed exploration of the three major segments of GPS-the space segment, control segment, and user segment-provides insights into the intricacies of satellite constellations, signal transmission, and the user's passive reception. The frequency plan and signal structure for GPS, GLONASS, and Galileo are examined, shedding light on the importance of spectrum allocation, modulation schemes, and signal coding in ensuring efficient and accurate navigation.

Furthermore, the research introduces the Multiplexed Binary Offset Carrier (MBOC) modulation scheme as a potential solution for second-generation radio navigation systems. The discussion outlines the qualities that a new modulation scheme should possess, such as robustness against interference, improved performance in code tracking, and shorter integration times.

In conclusion, the journey through the historical development of wavelet theory has revealed significant milestones, from Haar's discovery of an orthonormal basis to the introduction of various wavelet bases by Daubechies, Gabor, and others. The evolution of wavelet theory has involved addressing challenges in time- frequency localization, signal reconstruction, and achieving a balance between time and frequency resolutions. Affine wavelets emerged as a versatile solution, allowing for flexibility in tiling the time- frequency plane and offering a trade-off between time and frequency resolutions based on specific application requirements. The concept of multi- resolution analysis (MRA) played a crucial role in understanding wavelet properties, leading to the formulation of wavelet bases and their applications in signal decomposition and reconstruction. The discrete wavelet transform (DWT) was introduced as an efficient method for reducing signal length and computational complexity, with applications ranging from signal processing to noise reduction. The integration of wavelet decomposition with FFT operations has proven beneficial in improving signal-to-noise ratio (SNR) and mitigating interference in various scenarios, and halves the PRN code offset and the Doppler offset bin. This implies a computational complexity of O(N) to O(N/4).

In this context, the research presented here focuses on the application of the discrete wavelet transform in signal processing and denoising. The study employs wavelet decomposition to shorten signal length and reduce computational complexity, demonstrating its efficacy in correlation processes. The choice of Haar and Cohen-Daubechies-Feauveau (CDF) wavelets in the simulation demonstrated the versatility of wavelet bases in maintaining the integrity of the signal characteristics. Overall, the exploration of wavelet theory and its practical applications highlight its significance in modern signal processing and analysis.

Acknowledgement

The authors are grateful to Dr. Tapan Misra and Dr. Arundhati Misra Ray, SAC, ISRO, for their valuable suggestions. The authors are also thankful to Dr. Amitabha Bhattacharya from IIT Kharagpur for his guidance throughout the project.

REFERENCES

1. Mallat S. A Wavelet Tour of Signal Processing. Amsterdam: Elsevier; 1999.
2. Evans AG, Swift ER, Cunningham JP, Hill RW, Blewitt G, Yunck TP, et al. The Global Positioning System Geodesy Odyssey. Navigation. 2002;49(1):7–33. doi:10.1002/j.2161-4296.2002.tb00252.x.
3. Kaplan ED, Hegarty C, editors. Understanding GPS/GNSS: Principles and Applications. 3rd ed. Norwood (MA): Artech House; 2017.
4. Samama N. Global Positioning: Technologies and Performance. Hoboken (NJ): John Wiley & Sons; 2008. doi:10.1002/9780470241912.
5. Bastide F, Julien O, Macabiau C, Roturier B. Analysis of L5/E5 acquisition, tracking and data demodulation thresholds. Proceedings of the 15th International Technical Meeting of the Satellite Division of the Institute of Navigation (ION GPS 2002); 2002 Sep 24–27; Portland, OR, USA. Manassas (VA): Institute of Navigation; 2002. p. 2196–2207.
6. Dutton L, Rumens D, Forrest W, Ruiz L. Galileo's services. Proceedings of the 15th International Technical Meeting of the Satellite Division of The Institute of Navigation (ION GPS 2002); 2002 Sep; Portland, OR, USA. Manassas (VA): Institute of Navigation; 2002. p. 249–257.
7. Betz JW, Goldstein DB. Candidate designs for an additional civil signal in GPS spectral bands. Proceedings of the 2002 National Technical Meeting of The Institute of Navigation; 2002 Jan 28–30; San Diego, CA, USA. Manassas (VA): Institute of Navigation; 2002. p. 622–631.
8. Hein GW, Avila-Rodriguez JA, Wallner S, Pratt AR, Owen J, Issler JL, et al. MBOC: The new optimized spreading modulation recommended for GALILEO L1 OS and GPS L1C. In: 2006 IEEE/ION Position, Location, and Navigation Symposium; 2006 Apr 25–27; San Diego, CA, USA. Piscataway (NJ): Institute of Electrical and Electronics Engineers; 2006. p. 883–892. doi:10.1109/PLANS.2006.1650688.
9. Xu F, Gao Y. A complexity reduced frequency domain receiver for Galileo and GPS L1 signals. J Glob Position Syst. 2009;8:124–134. doi:10.5081/jgps.8.2.124.
10. Lei N, Zhu H, Cui J. Wavelet-based method for weak satellite signal acquisition. Proceedings of the 2011 International Conference on Transportation, Mechanical, and Electrical Engineering (TMEE); 2011 Dec; Changchun, China. Piscataway (NJ): Institute of Electrical and Electronics Engineers; 2011. p. 2487–2490.
11. Chang CL, Shou HN, Juang JC. Wavelet-based method for signal acquisition in GNSS receivers. In: SICE Annual Conference 2010; 2010 Aug 18–21; Taipei, Taiwan. Piscataway (NJ): Institute of Electrical and Electronics Engineers; 2010. p. 1261–1264.

